2010 NDIA GROUND VEHICLE SYSTEMS ENGINEERING AND TECHNOLOGY SYMPOSIUM
POWER & ENERGY MINI-SYMPOSIUM
AUGUST 17-19 DEARBORN, MICHIGAN

DEVELOPMENT OF HEAT PIPE LOOP TECHNOLOGY FOR MILITARY VEHICLE ELECTRONICS COOLING

Xudong Tang, PhD
Advanced Cooling Technologies, Inc.
1046 New Holland Ave, Lancaster PA 17601

Jon Zuo, PhD
Advanced Cooling Technologies, Inc.
1046 New Holland Ave, Lancaster PA 17601

Mary Goryca
U.S. Army RDECOM-TARDEC
6501 E. 11 Mile Road, Warren, MI 48397

ABSTRACT

Current standard military vehicle thermal management systems are based on single phase air/liquid cooling. To meet increasingly stringent demands for high power electronics thermal control, two-phase cooling solutions show great potential and can satisfy the need for compact and high heat flux heat acquisition, transport and dissipation under vibration and shock conditions. One novel two-phase cooling technology that has been developed in this work is a new Heat Pipe Loop (HPL), which exploits the advantages of both heat pipes and loop heat pipes while eliminating their shortcomings. Similar to heat pipes and loop heat pipes, the HPL operates on evaporation and condensation of a working fluid and uses capillary forces in the wick for the fluid circulation. Unlike in a heat pipe, the liquid and vapor in the HPL flow in separate passages made from smooth wall tubing. This results in a low pressure drop and consequently great heat transfer capacity and distance over which the heat can be transferred. The evaporator wick in a HPL is also made in-situ through a low cost manufacturing process and has a high thermal conductance, much like the low cost traditional heat pipe wick. To demonstrate the HPL technology, a compact 3kW HPL thermal management system was successfully designed, built and tested in an environment representative of military combat vehicles. This system consisted of six compact plug-and-play HPL modules. Each HPL module was designed to transport 500W of waste heat from two discrete high power devices on an electronics board to a chassis level thermal bus that was a pumped liquid loop. The HPL evaporator (or heat source) temperature was maintained below 80°C with a heat sink temperature of 30-50°C. The advantages of the HPL technology include: (1) Passive operation and high reliability; (2) Low cost in-situ wick fabrication; (3) High conductivity evaporator wicks; (4) Long distance heat transfer capability; and (5) Insensitivity to vibration/shock and gravitational orientation.

INTRODUCTION

It is becoming increasingly common to mount vehicle powertrain electronics directly onto the internal combustion engines and transmissions instead of the traditional locations inside the passenger compartment. The new packaging trend aims to shorten the connection wires between the electronic components and the control objects, accomplishing more compact and cost-effective packaging with greater design flexibility. However, this approach introduces vibration-induced issues to the powertrain electronics, which eventually can deteriorate the structural and cooling performance of the electronics.

From the data available [1], the vibration conditions in commercial automobiles ranges from 10 Grms (root-mean-square of acceleration) on the engine and transmission to 3-5 Grms in the passenger compartment. Unlike commercial vehicles, military combat vehicles may have additional shock sources from gun firing, ballistic launch and abrupt maneuvering. The mechanical shock environment in combat vehicles is classified as Basic, Gun Firing, Operational Ballistic or High Intensity. A “Basic” shock can be at 30 G in an 11 ms half-sine wave, while a “High Intensity” shock can be 1,200 G in a 1 ms half-sine wave.

Heat pipes have become a commonly used technology for electronics cooling, because of their high thermal conductance, inherent simplicity, passive operation and high reliability. However, heat pipes are limited in their heat transfer capacity and distance, because of the pressure drop

in the liquid flow in the thin annular. Loop heat pipes (LHP), an emerging technology for satellite thermal control, are orders of magnitude more capable in heat transfer capacity and distance than heat pipes [2-4]. Some recent efforts have been made to "transition" the LHP technology to terrestrial electronics cooling [5-6]. In general, LHPs require precision machining and integration of fine pore wicks. This is a significant cost driver and inhibitor for high volume application of such devices.

As mentioned, the shock and vibration experienced in commercial and military applications pose significant challenges and can adversely affect the performance of passive capillary-driven devices, such as heat pipes and LHPs. Resonant vibrations, for example, can break the liquid-vapor meniscus in the evaporator wick resulting in poor performance. Mechanical shocks may also disturb the fluid distribution in the hydraulic lines of the two-phase loop. This is important because the fluid distribution greatly affects the start up behavior and long-term operating characteristics of a LHP. While short transients may not have a significant impact, large amplitude and periodic shocks can displace the liquid and alter the performance of the loop for an extended period of time. Large mechanical shocks can also damage the internal structure of the LHP evaporator such as the knife-edge seal.

In the work presented in this paper, the development of a novel capillary-driven two-phase electronics cooling technology named the Heat Pipe Loop (HPL) was described, which adopts the advantages of both the heat pipe and loop heat pipe designs while eliminating their shortcomings. The operating principle and heat transfer performance under vibration and shock environments is also discussed. A 3kW electronics cabinet thermal management system with six plug-and-play HPL modules was successfully demonstrated where each HPL module could transport 500W from two discrete high power devices on an electronics board to a chassis level thermal bus.

NOMENCLATURE

A_{wick}	wick cross-sectional area (m^2)
D	transportation line diameter (m)
f	friction factor
K_{wick}	wick permeability (m^2)
L	transportation line length (m)
L_{wick}	wick effective length (m)
$\dot{m}$	mass flowrate (kg/s)
P_{cap}	capillary pressure (Pa)
Re	Reynolds number
r_{wick}	mean pore radius (m)
ρ	density (kg/m^3)
σ	surface tension (N/m)
ΔP	HPL loop pressure drop (Pa)
ΔP_{wick}	porous wick pressure drop (Pa)
μ	liquid dynamic viscosity (Pa s)
ΔP_{wick}	porous wick pressure drop (Pa)
μ	liquid dynamic viscosity (Pa s)

HPL WORKING PRINCIPLE

Figure 1 illustrates the basic concept of the HPL technology, which is U.S. patent pending. The HPL consists of the following components: a capillary evaporator (responsible for generating the capillary forces that drive the working fluid), a condenser, a liquid reservoir (to ensure a reliable startup), and liquid and vapor transport lines. Similar to heat pipes and LHP's, the HPL relies on the evaporation and condensation of a working fluid and uses the capillary forces in the wick for the fluid circulation. The heat applied to the evaporator vaporizes the working fluid in the wick. Driven by the vapor pressure, the vapor flows through the smooth vapor line and enters the condenser. In the condenser, the vapor is cooled and condenses into liquid, which is sent back to the reservoir via the liquid line. The capillary pressure generated by the liquid/vapor interface (meniscus) in the evaporator wick surface provides the pumping force that delivers the working fluid to the wick. The maximum capillary pumping pressure in the evaporator wick and the fluid pressure drop in the loop determine the heat transfer capability of the HPL. To ensure the evaporator wick is always in contact with the working fluid, the volume of the reservoir and the working fluid inventory need to be carefully designed. This is important to guarantee that the startup of the HPL is reliable under all operation conditions.

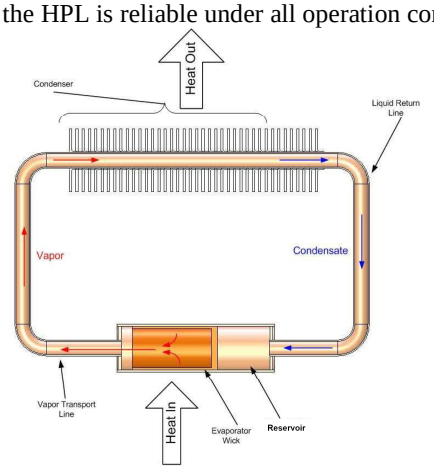

Figure 1. Concept of the heat pipe loop (HPL)

In contrast to a traditional heat pipe, the liquid and vapor in a HPL flow in separate lines that are made of wickless, smooth wall tubing (low pressure drop), which enhances the

heat transfer capacity and distance over which heat is transfer. Also, the evaporator wick in a HPL, unlike that used in a loop heat pipe, is an in-situ made, high thermal conductance, non-inverted meniscus wick, which improves the evaporator thermal conductance and reduces the manufacturing cost.

The HPL developed in this work used copper as the envelope material and water as the working fluid. The evaporator was a cylindrical copper tube (0.75" OD) with a sintered copper powder primary wick. The reservoir was integrated with the evaporator and the liquid stored in the reservoir was delivered to the heat zone by the primary wick capillary. The liquid in the evaporator absorbed the heat. The vapor exited the evaporator and entered a 0.25" OD vapor line. The vapor was subsequently condensed and the returning liquid from the condenser flowed through a 0.25" OD "bayonet" tubing to the primary wick before entering the reservoir. A phosphor bronze screen secondary wick attached on the bayonet tubing was used to ensure the continuous liquid supply to the primary wick under all operating conditions, including cold startup, rapid heat load variation, and gravitational orientation variation. A copper baffle with punctuated holes was incorporated inside the reservoir to restrict the liquid "churning motion" generated by vibrations.

Table 1. Specifications of the HPL

Evaporator OD (in)	0.75
Reservoir Volume (cc)	15.7
Vapor Line OD (in)	0.25
Vapor Line Length (in)	2.6
Liquid Line OD (in)	0.25
Liquid Line Length (in)	16.5
Condenser ID (in)	0.25
Condenser Length (in)	6
Heat Zone Length (in)	1.0
Wick Thickness (in)	0.056
Wick Pore Radius (μm)	28
Wick Permeability (m^2)	5.83×10^{-12}
Wick Porosity	40%

The detailed specifications of the HPL are listed in Table 1. The HPL heat transport performance is determined by the balance between the capillary pressure provided by the primary wick and the overall pressure drop in the loop.

The major pressure drop in the HPL is due to the liquid flow in the porous primary wick, defined by Darcy's Law.

$$\Delta P_{wick} = \frac{\mu L_{wick}\dot{m}}{\rho K_{wick} A_{wick}} \quad (1)$$

while the pressure drop in the vapor or liquid line can be calculated as:

$$\Delta P = f(\mathrm{Re})\rho\frac{v^2 l}{2D} \quad (2)$$

The capillary pressure is a function of the wick pore radius and the liquid surface tension:

$$P_{cap} = \frac{2\sigma}{r_{wick}} \quad (3)$$

Based on the wick properties and HPL geometries listed in Table 1, the HPL should be able to transfer heat up to 280W and maintain the evaporator temperature at 68°C with a 50°C heat sink.

HPL SYSTEM DESCRIPTION

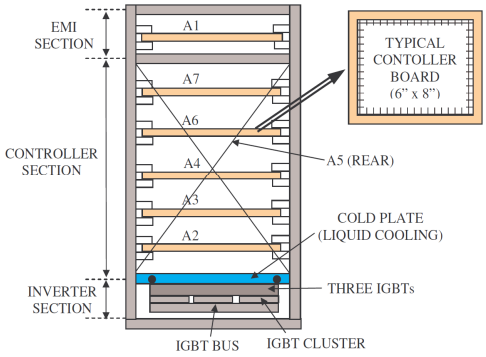

Figure 2. Typical layout of the electronic controller/inverter box for an Army FCS

A typical electronic controller/inverter box for a representative FCS (Future Combat System) has seven electronics circuit boards as illustrated in Figure 2 [1] where each controller board typically has a 6 inch × 8 inch footprint. The controller board is attached to a chassis by wedge-locks with a mounting pitch height of approximately 1.0 inch. The waste heat generated by these electronics boards is dissipated mainly by air convection, which becomes more and more incompetent with fast development of high power electronics.

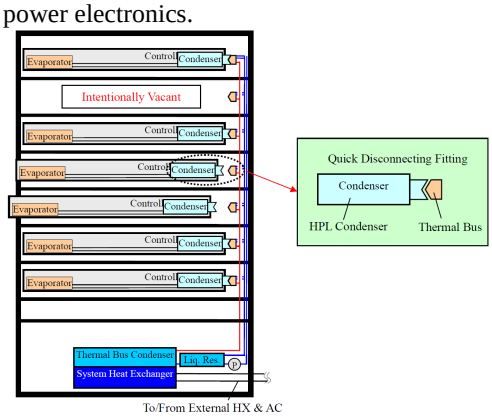

Figure 3. Thermal architecture of an HPL electronics cabinet cooling system

To address the future cooling requirements in the FCS electronics cabinet, a new thermal architecture is used as shown in Figure 3. Each circuit board has an associated HPL cooling module that is used to collect waste heat from high power components in the board and transport the heat to the chassis. The HPL employs also has 'plug-and-play' thermal connector that mates with the cabinet chassis thermal bus. This allows the circuit boards to be conveniently installed and removed from the chassis, making the thermal connections with the same ease as the electrical connections. The cabinet chassis thermal bus is a Pumped Liquid Loop that receives the heat from HPL's and rejects the total heat to a system heat exchanger.

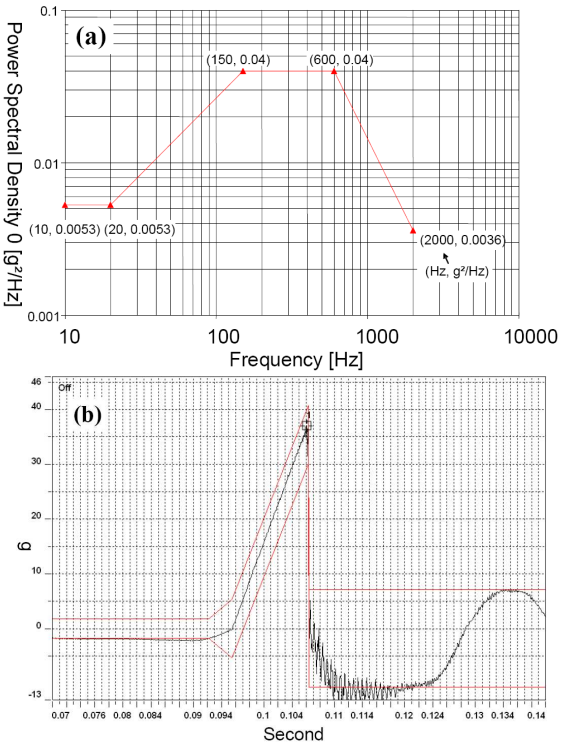

Figure 4. Typical (a) vibration and (b) Shock Profiles of FSC-Variant Body/Frame Mounted Components [1]

The FSC-Variant Body/Frame Mounted Components also must be able to sustain significant vibrations and shocks during normal operations. Figure 4(a) shows a representative PSD profile of the vehicle's body and frame in a FCS-like military vehicle. The PSD curve produces a maximum vibration level of about 5 Grms. Figure 4(b) shows the shock profile of the same vehicle with a half-sine pulse of 40 Gpeak for 10-15 ms. Clearly, the FCS electronics cabinet and the HPL cooling system will have to function properly when subjected to these vibration/shock profiles.

TEST APPARATUS

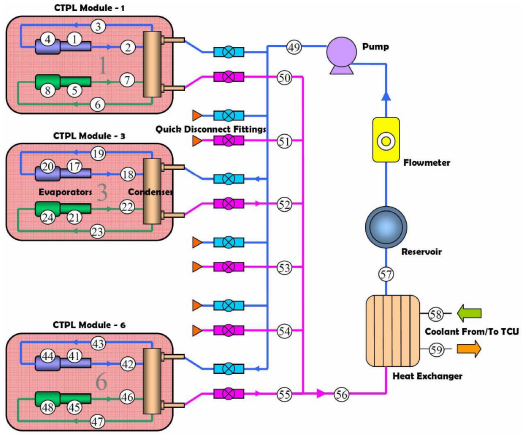

Figure 5. Schematic of a 3kW HPL electronics cabinet cooling system

A schematic 3kW HPL thermal management system designed for electronics cabinet cooling (with three of the six 500W HPL modules) is shown in Figure 5. The numbers in the figure represent the thermocouple locations. The HPL cooling system consists of one pumped liquid loop and six parallel connected 'plug-and-play' HPL modules. The HPL modules acquire heat from the discrete mockup electronics board heat sources, and transfer the heat to the condensers that were thermally coupled with the pumped liquid loop. The pumped liquid loop acts as a cabinet chassis level thermal bus that receives heat from the HPL modules and rejects the total amount of heat to the system heat exchanger. The pumped liquid loop includes: a heat exchanger, a reservoir, a flowmeter, a gear pump and manifolds that collect the coolant from the HPL modules. A flatplate heat exchanger (FG3X8-24) transfers heat between the pumped liquid loop coolant and a constant temperature coolant supplied from an exterior Temperature Control Unit (TCU) that simulates the working environment. In our tests, the pumped liquid loop coolant flowrate was monitored by the flowmeter (Omega FPR 312) and controlled by the DC voltage supplied to the gear pump (Hopkins-Carter Jabsco 24V Water Pump).

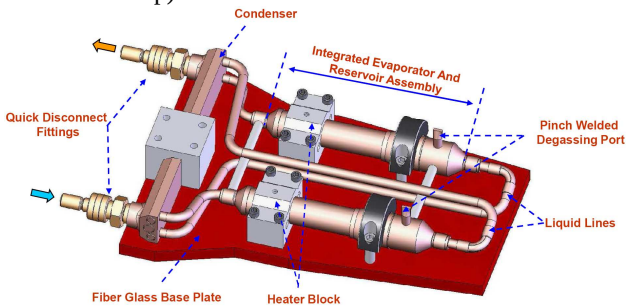

Figure 6. Solid model of individual 500W HPL module

Figure 6 shows the 500W HPL module solid model. Due to the limited space inside the electronics cabinet and rough vibration/shock working environment, the HPL module must be compact and the mass must be minimized while maintaining the structural integrity. The HPL module was mounted on a 7" by 10" supporting fiber glass plate where each module consisted of two separated 250W HPL's. Two 1" long saddle shape aluminum heater blocks with embedded electric cartridge heaters simulated the electronics board high power heat sources and were clamped on the 0.75" O.D. HPL evaporators. The reservoirs were integrated with the evaporators to further reduce the system size.

In our design, the two evaporators in each HPL module had their own separate vapor/liquid transport lines and shared the same condenser, yet there was no physical fluid communication between the two loops. The sharing of the condenser was simply mechanical and structural. The condenser was made of copper with three (3) parallel internal channels that were 6" in length. The liquid coolant from the chassis thermal bus flowed through the middle channel that was connected to the quick disconnect fittings shown in Figure 7. The counterflow vapor from the two loops was subsequently cooled and condensed in the other two channels in the condenser.

The condenser was installed on the chassis side of the HPL module and outfitted with quick-disconnect fittings for the liquid coolant inlet and outlet such that it could be easily plugged into or disconnected from the thermal bus, i.e. the pumped liquid loop manifold. This versatile design enables the heat acquired by HPL modules to be readily transferred to the pumped liquid loop.

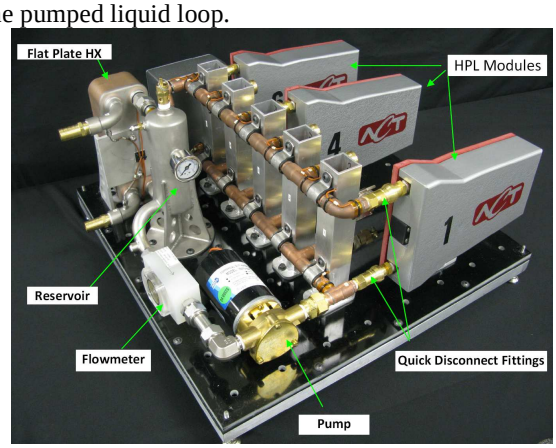

Figure 7. The 3kW HPL system for electronics cabinet cooling with 3 HPL modules installed

Figure 7 shows the test setup for a 3kW HPL electronics cabinet cooling system. The entire system was packaged with 24 inch x 24" inch footprint that was 12 inches tall. The HPL modules were also covered with foam for thermal insulation. All the components were hard mounted on a Garolite base plate supported by aluminum frames. The lower manifold of the pumped liquid loop distributed the cooling water into the modules while the upper manifold collected the warm water from each module and directed it into the Flat Plate heat exchanger.

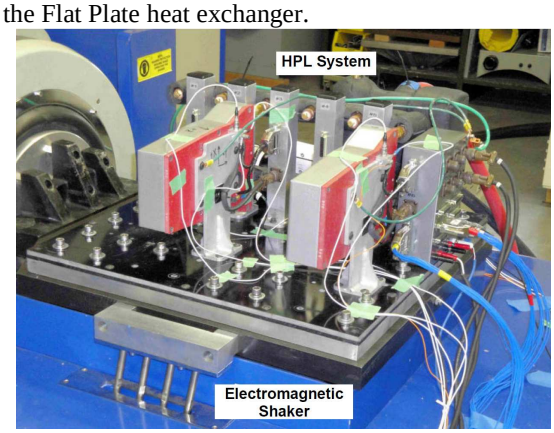

Figure 8. The 3kW HPL system mounted to an electromagnetic shaker for vibration/shock tests.

Instruments including accelerometers and thermocouples were carefully installed to provide accurate characterization of the transient system/component level thermal response and the vibration/shock spectrum during thermal cycle testing. The system was then mounted to an electromagnetic shaker table as shown in Figure 8. The positions of the thermocouples are shown in Figure 5.

A typical thermal cycle test of the HPL system began with a cold system. The heat supply was turned on, and followed by subsequent increase in the heat load after the temperature realized. The maximum heat load applied on each HPL module was 500W. Each individual HPL loop in each module had up to 250W load. The system heat sink temperature was constant during the testing. Thermal cycle tests were also performed while the HPL system was subjected to a vibration/shock environment (specified in Figure 4) generated by the electromagnetic shaker. The vibration in one of the three space directions was continuously applied on the HPL during the entire thermal cycle tests. The shocks were applied in a discrete manner: one shock per minute with alternative +/- polarities. Orientation tests of the HPL module were conducted at four different space orientations:

(1) Nominal, as shown in Figure 7.
(2) Horizontal, where all the components in the HPL module were at the same elevation.
(3) Vertical-1, where the evaporators were vertically oriented and the condenser was on the top.
(4) Vertical-2, where the evaporators were vertically oriental and the condenser was at the bottom.

TEST RESULTS

Most of tests of the HPL cooling system were performed in the nominal orientation. The same heat load was provided to each electric heater. The heat sink temperature was set to 50°C simulating the hottest working environment. The maximum heat transfer capabilities and the corresponding evaporator temperature are listed in Table 2.

Table 2. Thermal performance of HPL modules with a fixed 50°C heat sink temperature; nominal orientation.

		Q_{max} (W)	Evap. Temp. (°C)
Mod-1	Evap101	500	72
	Evap102		68
Mod-2	Evap201	520	74
	Evap202		74
Mod-3	Evap301	540	75
	Evap302		73
Mod-4	Evap401	510	73
	Evap402		76
Mod-5	Evap501	520	74
	Evap502		70
Mod-6	Evap601	500	75
	Evap602		74

From this baseline data, it can be concluded that the maximum heat load and heat flux on each HPL evaporator can reach 250-270W. The maximum heat flux can be applied on the evaporator is 30W/cm^2. Each HPL module also was able to reject heat up to Q_{max} = 500-540W such that a 6 module HPL cooling system could achieve the 3kW electronics cabinet cooling requirement without evaporator dryout and system overheating. The evaporator temperature was able to be maintained between 68-76°C, below the electronics junction temperature limit. The temperature difference between evaporators within one module was mostly due to the variation of the wick pore sizes and permeabilities, caused by the fabrication inconsistencies. It should also be noted that the test results agreed very well with the thermal model predictions reported in the previous section.

Thermal cycle tests of one of the six HPL modules were shown below. The HPL module with a heat load up to 500W was tested under stationary, vibration and shock conditions. The temperature variations during these tests are shown in Figure 9, 11 and 12, respectively. It can be seen that the evaporator temperature stabilized in a very short period of time although subject to a rapid heat load variation. No noticeable temperature fluctuations were observed during this transient heating period.

The evaporator temperature was highest in the HPL loop. The next highest temperature was in the vapor. The temperature difference between them was determined by the evaporator wick thermal resistance and the heat flux applied. The condenser not only turned the vapor to the liquid, but also provided additional subcooling to compensate the heat leak from the evaporator to the reservoir. Therefore, the returned liquid had a cooler temperature than the condenser inlet vapor temperature. After the liquid returned to the reservoir, it was again heated by the evaporator heat leak and its temperature was raised to the saturation temperature.

The HPL showed very good temperature repeatability when identical heat loads were applied. In the stationary tests, the temperature of the (two) evaporators was stabilized at 70°C with 400W during the heat load ramping up, and the temperature returned to roughly the same value after the heat load was decreased to 400W. Similar trends were also observed in the vibration/shock tests.

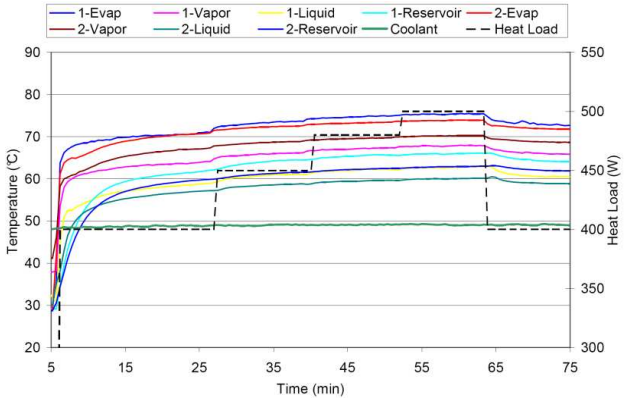

Figure 9. Stationary thermal cycle test of HPL in "Nominal" orientation, 50°C heat sink

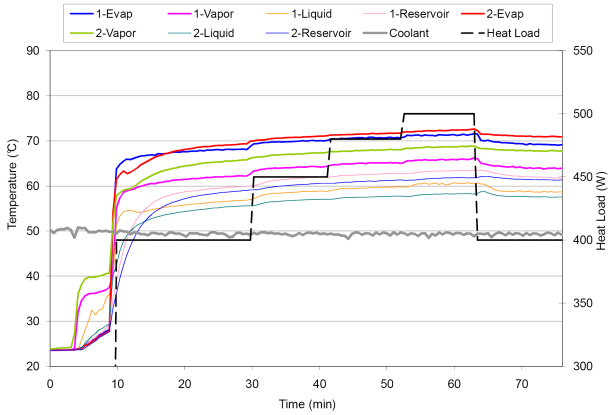

Figure 10. Vibration thermal cycle test of HPL in "Nominal" orientation, 50°C heat sink

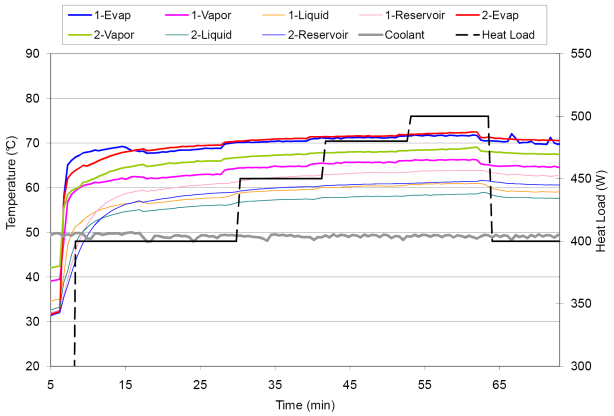

Figure 11. Shock thermal cycle test of HPL in "Nominal" orientation, 50°C heat sink

The vibration/shock working environment had minimum impact on the HPL system thermal performance. No significant structural damage was observed after long term vibration/shock operation. In the particular case shown in Figure 9, 11 and 12, the HPL module achieved 500W heat dissipation under vibration/shock conditions and the evaporators temperatures were similar. However, some of the evaporators in other HPL modules showed reduced Q_{max} when vibration/shock was applied. This was partly due to the evaporator wick fabrication inconsistency. Another contributing factor may have been the meniscus disturbance caused by the vibration/shock that in turn may have reduced the capillary pressure.

Additional tests with more intensive vibration/shock, e.g., 24 Grms vibration or 123 G_{peak}, the HPL modules still functioned properly without significant degradation in their performance.

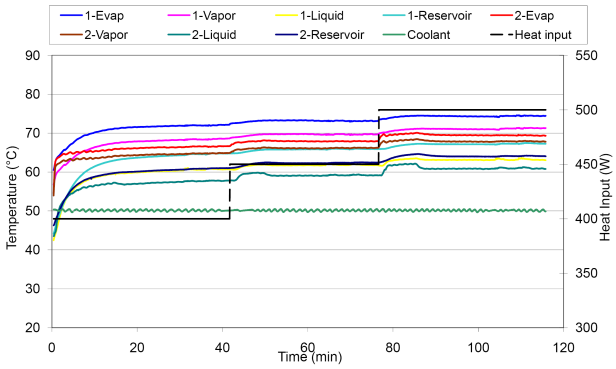

Figure 12. Thermal cycle test of HPL module in "Horizontal" orientation, 50°C heat sink

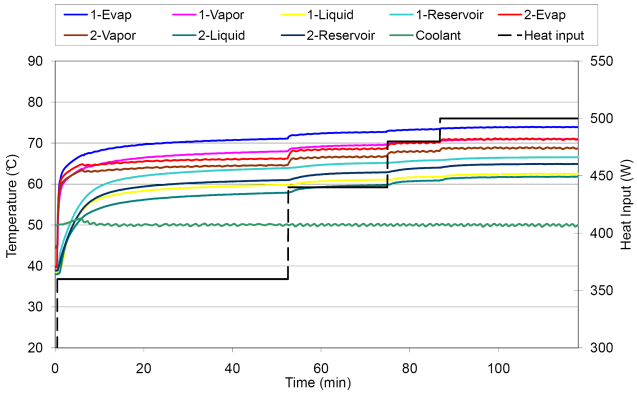

Figure 13. Thermal cycle test of HPL module in "Vertical-1" orientation, 50°C heat sink

As mentioned, orientation tests of the HPL system were conducted in four space orientations. When the HPL module was in the "Veritcal-1" orientation, the loop was working under a gravity-aided situation, i.e., the liquid working fluid in the condenser was stored at a higher elevation than that in the evaporator. The additional pressure head of the working fluid assisted the capillary pressure in circulation of the fluid in the loop. However, the liquid supply from the reservoir to the primary wick became purely relied on the capillary flow from the secondary wick. On the contrary, when the HPL module was in the "Veritcal-2" orientation, the loop circulation became working against the gravity. But the liquid pool in the reservoir ensured the primary wick was always in contact with the liquid and provided extra gravity to help the capillary.

The test results showed similar heat transfer performance and temperature characteristics in all four orientations. This demonstrates the insensitivity of the HPL system to orientation. The results of a HPL module in the "Horizontal" and "Vertical-1" orientations are shown in Figure 12 and Figure 13, respectively. Both were tested up to 500W and did not reach the capillary limit. Both systems demonstrated similar steady-state and transient behavior.

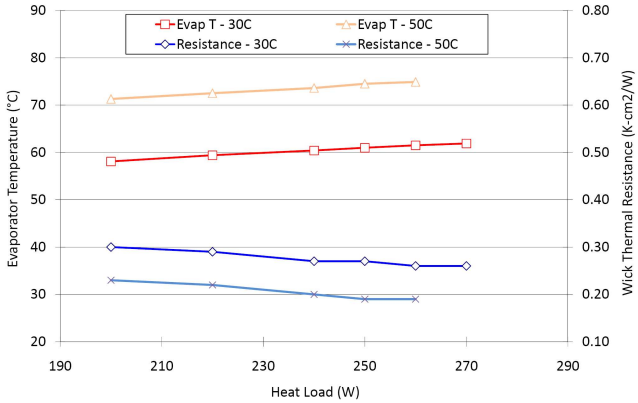

Figure 14. Heat load dependences of the evaporator temperature and wick thermal resistance

The HPL evaporator temperature and wick thermal resistance at various heat loads and heat sink temperature (30°C and 50°) are shown in Figure 14. The wick thermal resistance was defined as the ratio of the temperature difference between the evaporator surface and the vapor divided by the heat flux.

The HPL had a slightly higher heat transfer capability at lower heat sink temperature; notably, Q_{max} = 270W at 30°C heat sink and Q_{max} = 260W at 50°C heat sink. In addition, the HPL operated at a higher temperature with higher heat sink temperatures. The evaporator temperature also increased with an increase in the heat load. For heat loads in the range of 200W to 250W, the evaporator temperature increased about 3.1°C in both cases due to the fixed length of the condenser that required higher vapor temperature to reject additional amount of the heat load.

As shown, the wick thermal resistance also decreased when the applied heat load increased. The wick thermal resistance ranged from 0.2-0.3 K-cm^2/W when the heat load reached the capillary limit, which is very close to the thermal resistance of traditional heat pipe wicks.

CONCLUSION

A 3kW electronics cabinet thermal management system with six plug-and-play HPL modules was successfully demonstrated. Each HPL module was able to transport 500W heat from two discrete heat sources, simulating high power devices on an electronics board, to a chassis level thermal bus while maintaining the evaporator below 80°C. The maximum heat flux of the HPL evaporators was 30W/cm^2.The HPL cooling system demonstrated desirable thermal management features, such as healthy cold startup, no temperature fluctuation during heat load variation transient, and good thermal repeatability. It has further been confirmed by experiment that the HPL cooling performance was not adversely affected by the vibration or shock for the conditions tested: Vibrations (5Grms, 0-2,000Hz) and shocks (40Gpeak in 10-15 ms). The HPL system operation was also insensitive to the gravitational orientation. The evaporator wick thermal resistance (flux-based) was 0.2-0.3 K-cm2/W similar to traditional heat pipe thermal resistances.

In summary, the HPL technology demonstrated: (1) passive operation and high reliability; (2)low cost in-situ wick fabrication; (3) high conductivity non-inverted evaporator wicks; (4) long distance heat transfer capability; and an (5) insensitivity to vibration/shock or gravitational orientation.

ACKNOWLEDGEMENTS

This work was supported by SBIR Phase II contract (#W56HZV-07-C-0514) from the U.S. Army RDECOM-TARDEC.

REFERENCES

[1] http://www.hamiltonsundstrand.com/, 2008

[2] Yu.F. Maydanik, 2003, “Loop Heat Pipes”, Applied Thermal Engineering, 25, 635-657

[3] R. J. McGlen, R. Jachuck, S. Lin, 2004, “Integrated thermal management techniques for high power electronic devices”, Applied Thermal Engineering , 24, 1143-1156

[4] V.G. Pastukhov , Yu.F. Maidanik, 2003, “Miniature loop heat pipes for electronics cooling”, Applied Thermal Engineering, 23, 1125-1135

[5] Yu. Maydanik, S. Vershinin, 2010, “Development and Investigation of Copper-Water LHP with High Operating Characteristics”, 15th IHPC

[6] V. PastukhovYu. Maydanik, 2010, “LHP-based coolers for graphics cards”, 15th IHPC